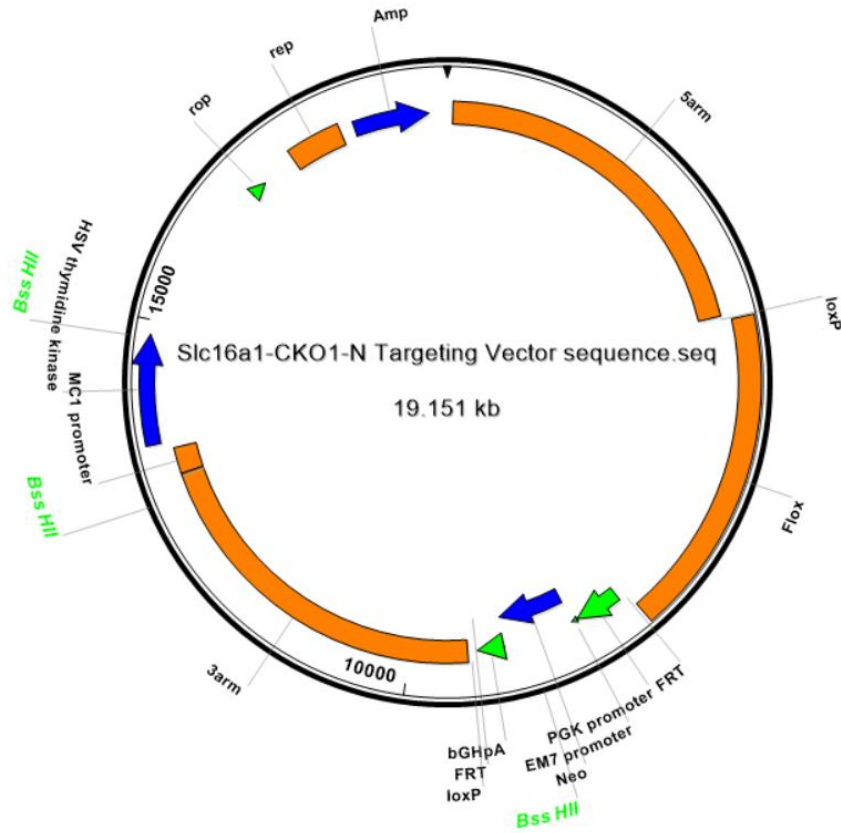


Supplemental Figures

A



B

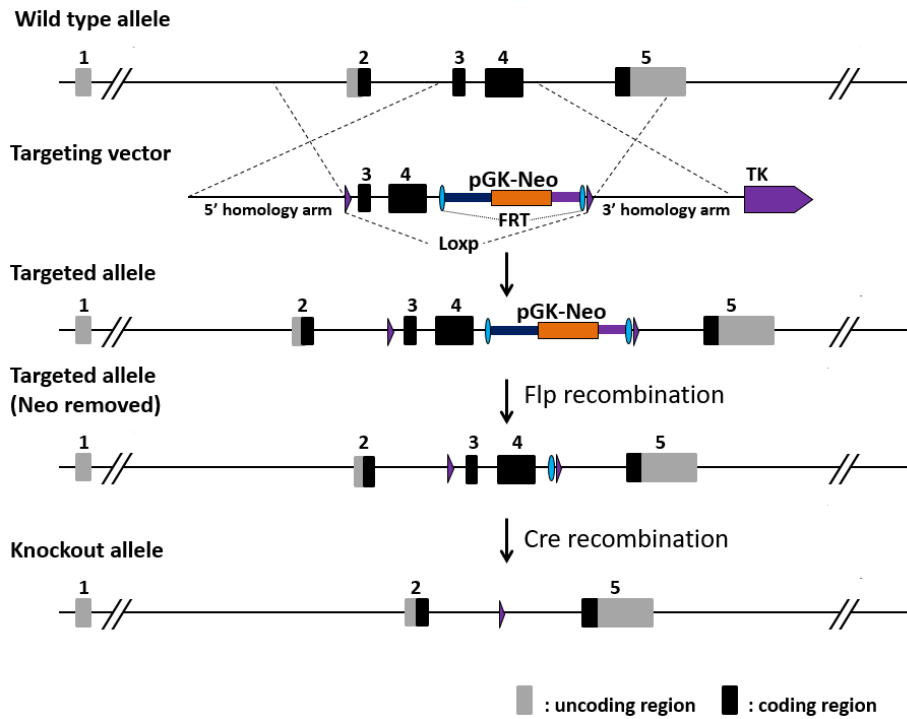


Figure S1. Details of the strategy for generation of the floxed *Slc16a1*-delete mice

- (A) The map of the plasmid used for homologous recombination for generation of floxed *Slc16a1*-deleted mice.
- (B) A diagram to depict the steps for generation of Cre-based conditional *Slc16a1*-deleted mice.

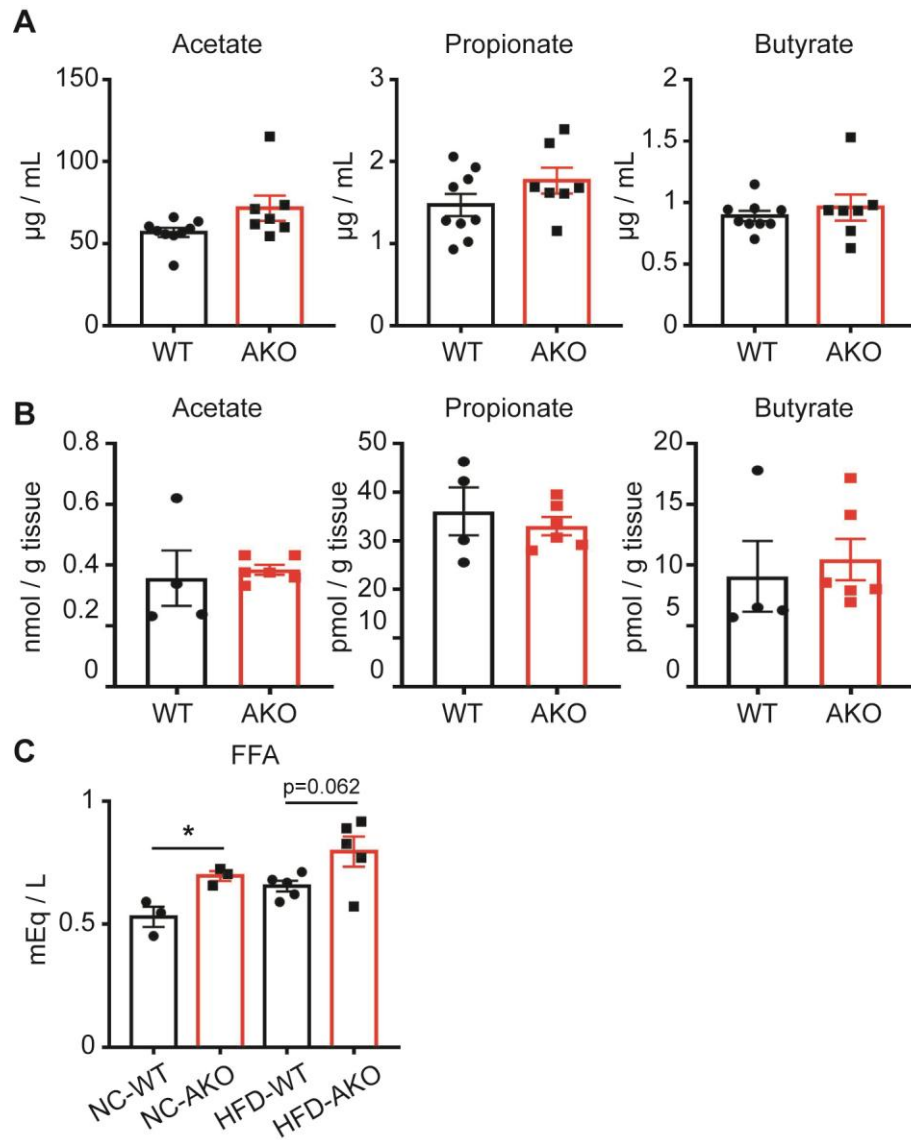


Figure S2. Analyses of short-chain fatty acids and free fatty acids in the *Slc16a1*-deleted mice

(A) Concentration of acetate, propionate and butyrate in the serum of the mice fed with HFD as described in Figure 2.

(B) Concentration of acetate, propionate and butyrate in the eWAT of the mice fed with HFD as described in Figure 2.

(C) Concentration of free fatty acids (FFA) in the serum of mice fed with normal chow or HFD as described in Figure 2.

The data are shown as mean \pm S.E.M., * for $P < 0.05$.

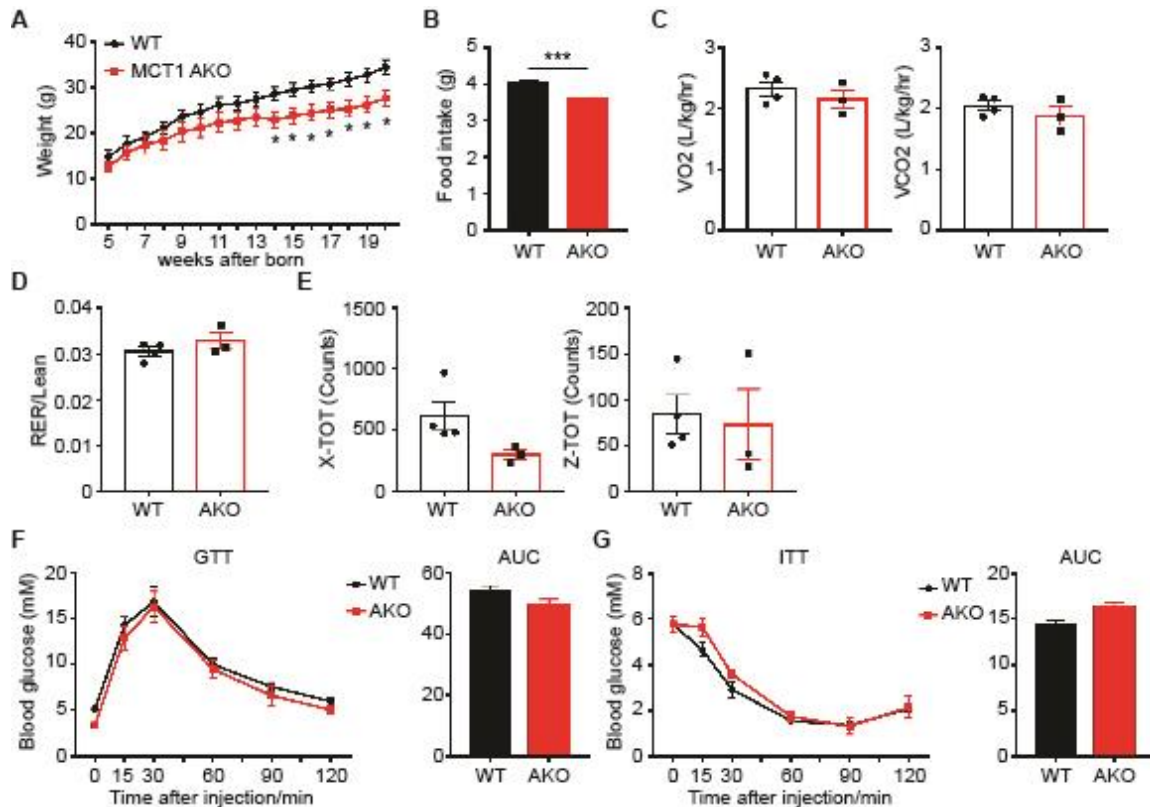


Figure S3. Analyses of *Slc16a1*-deleted mice under normal chow

- (A) Body weight of the mice fed with normal chow for 19 weeks ($n = 5$ for each group).
- (B) Food intake of the mice.
- (C) Oxygen consumption and carbon dioxide production of the mice.
- (D) Respiratory exchange rate (RER) of the mice. The rate was normalized with lean weight.
- (E) Movement of the mice on X and Z axes. The data in C-E were measured during a 24-hour period including a light and dark cycle.
- (F) Glucose tolerance tests (GTT) of the mice. Area under curve (AUC) is shown on the right.
- (G) Insulin tolerance tests (ITT) of the mice. AUC is shown on the right.
- WT, *Slc16a1^{fl/fl}* mice; AKO, *Slc16a1^{fl/fl}aP2-Cre^{+/-}* mice. All the quantitative data are shown as mean \pm S.E.M., * for $P < 0.05$ and *** for $P < 0.001$.

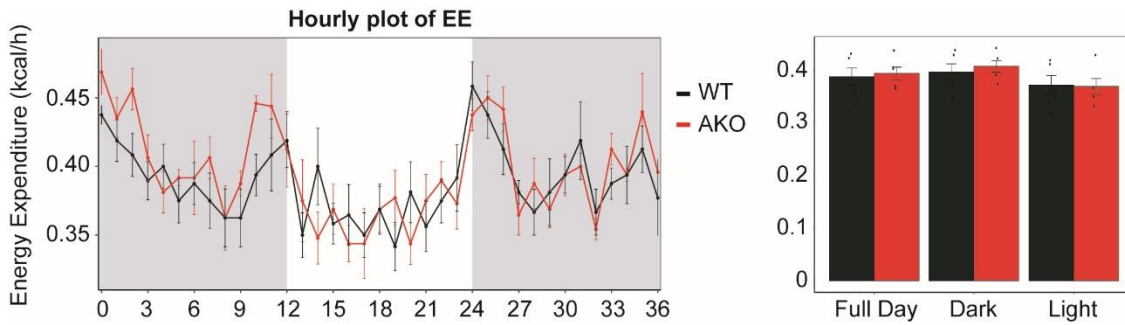


Figure S4. Energy expenditure (EE) of the HFD mice using CalR method

Left, hourly plot of EE. Right, average statistic of EE. The CLAMS data from metabolic cage were uploaded to CalR website (<https://CalRapp.org>) for analysis and picture generation.

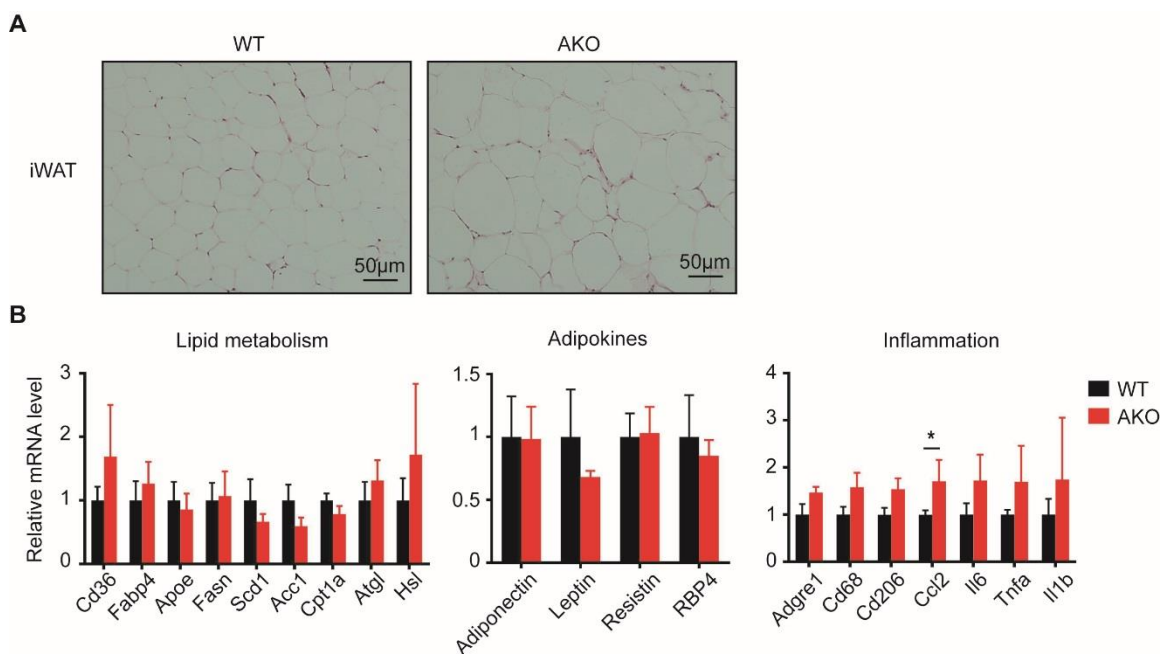


Figure S5. Analyses of iWAT in the mice fed with HFD

(A) Representative images of H&E staining of iWAT of the mice as described in Figure 2.

(B) Relative mRNA levels of genes involved in lipid metabolism, adipokines and inflammation in the iWAT of the mice.

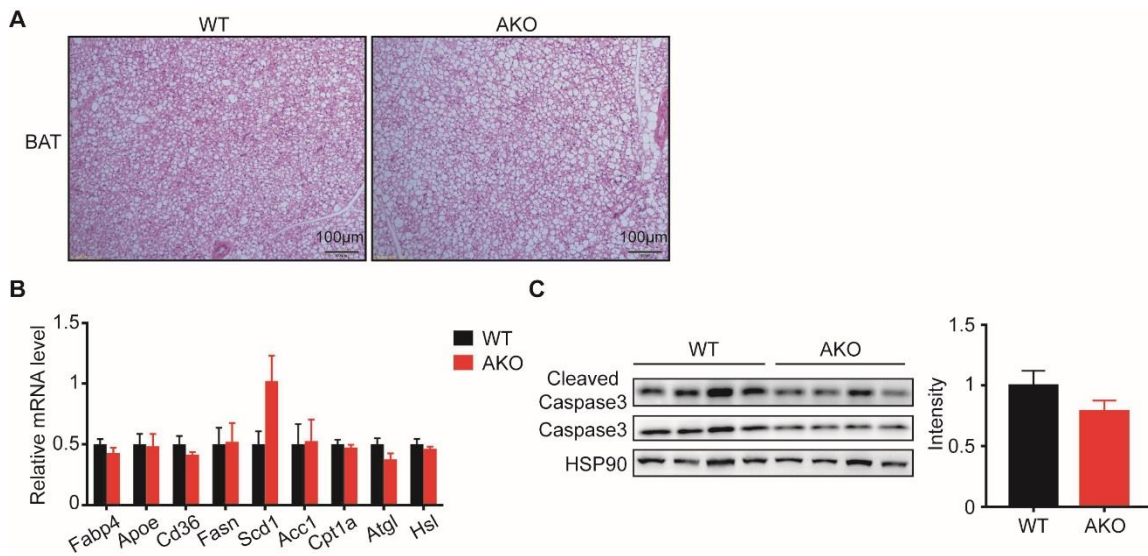


Figure S6. Analyses of BAT in the mice fed with HFD

(A) Representative images of H&E staining of BAT of the mice as described in Figure 2.

(B) Relative mRNA levels of genes involved in lipid metabolism.

(C) Western blotting to detect cleaved caspase 3 in BAT of the mice. Quantification of cleaved caspase 3 relative to HSP is shown on the right.

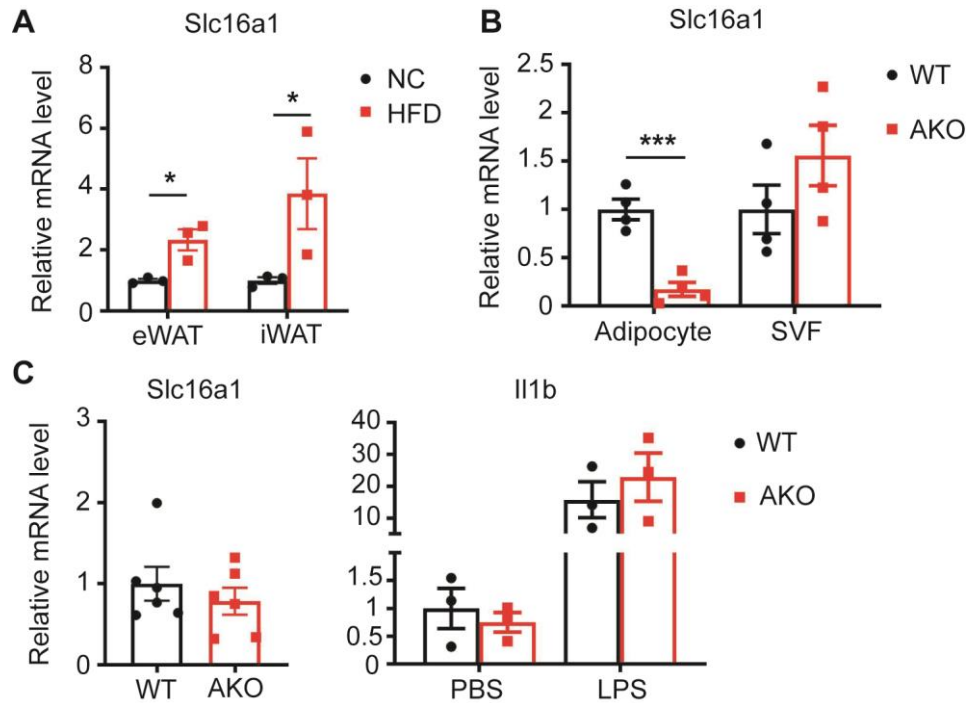


Figure S7. Analyses of Slc16a1 and Il1b expression

(A) Relative mRNA level of Slc16a1 in eWAT and iWAT under normal chow (NC) and HFD conditions (n = 3 for each group).

(B) Relative mRNA level of Slc16a1 in adipocyte and SVFs derived from eWAT (n = 4 for each group).

(C) Left, relative mRNA level of Slc16a1 in peritoneal macrophages from WT and AKO mice (n = 6 for each group). Right, relative mRNA level of Il1b in peritoneal macrophages stimulated with 100ng/mL LPS for 12 hours (n = 3 for each group).

Quantitative RT-PCR was used to analyze the mRNA levels. Data are shown as mean \pm S.E.M., * for P < 0.05, *** for P < 0.001.